Interaction of ICMEs with the Solar Wind

Pascal Démoulin

Observatoire de Paris, LESIA, UMR 8109 (CNRS), F-92195 Meudon Principal Cedex, France

Abstract. Interplanetary Coronal Mass Ejections (ICMEs) are formed of plasma and magnetic field launched from the Sun into the Solar Wind (SW). These coherent magnetic structures, frequently formed by a flux rope, interact strongly with the SW. Such interaction is reviewed by comparing the results obtained from *in situ* observations and with numerical simulations. Like fast ships in the ocean, fast ICMEs drive an extended shock in front. However, their interaction with the SW is much more complex than that of the ship analogy. For example, as they expand in all directions while traveling away from the Sun, a sheath of SW plasma and magnetic field accumulates in front, which partially reconnects with the ICME magnetic field. Furthermore, not only ICMEs have a profound impact on the heliosphere, but the type of SW encountered by an ICME has an important impact on its evolution (*e.g.* increase of mass, global deceleration, lost of magnetic flux and helicity, distortion of the configuration).

Keywords: Coronal Mass Ejections, Magnetic cloud, Magnetic field, Solar Wind
PACS: 96.50.Uv, 96.60.ph, 96.60.Vg

1. INTRODUCTION

The evolution of an ICME in the SW is part of a long series of physical processes (figure 1). It starts with the amplification of the magnetic field deep in the convective zone and its storage just underneath. At some point, the magnetic field becomes buoyantly unstable, a twisted flux rope is formed, it crosses the convective zone and then emerges at the photospheric level. This field is then processed and stored for a few days to a few weeks in the corona, before getting unstable and forming a new flux rope which is ejected from the Sun as a CME.

Despite the difference of medium, there are many physical analogies between an ocean and the SW (figure 2). So, St Malo was an idea place to get inspiration! In particular, fast moving objects are present in both media. They drive forward shocks which extend on a much larger scale than the moving object itself (see *e.g.* the MHD simulations of [1, 2, 3]).

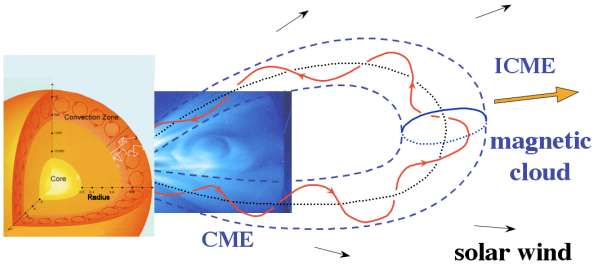

FIGURE 1. Schema showing the launch of a coronal mass ejection (CME) from the Sun. The CME is detected few days later in the interplanetary space as an ICME or a magnetic cloud (with a flux rope topology, as shown schematically). The image is from SOHO/LASCO.

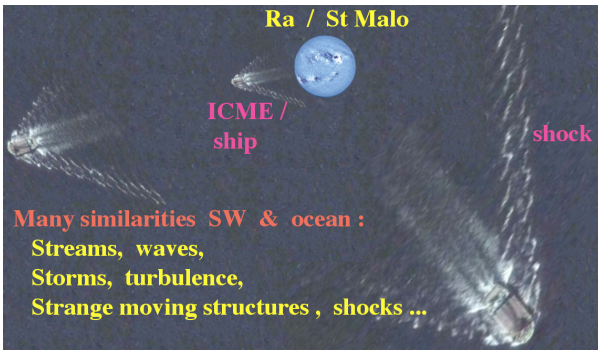

FIGURE 2. Analogies between CMEs / ships traveling in the SW / ocean. Compare the shock extension / shape to the one found in MHD simulations (*e.g.* figures 7a, 8 and 10a).

ICMEs are defined by one or several criteria depending on authors [*e.g.* 4, 5, 6]. Typical criteria are: (1) a proton temperature at least lower by a factor 2 for the SW with the same velocity; (2) an enhanced helium abundance (He/H $\geq$ 6%); (3) the presence of counter-streaming suprathermal ($>$ 80 eV) electron beams; (4) enhanced ion charge states; (5) a stronger magnetic field with lower variance than in the surrounding SW; (6) a low proton plasma β_p ($<$ 0.1); (7) a smooth and large rotation of the magnetic field. Magnetic clouds (MCs) are a sub-class of ICMEs with all criteria (1,5,6,7) satisfied. Their magnetic configuration, a flux rope, and their physical properties are typically better understood (but still partially!) than for the broader class of ICMEs.

A main difference between ships and ICMEs is that ICMEs are strongly affected by their surrounding

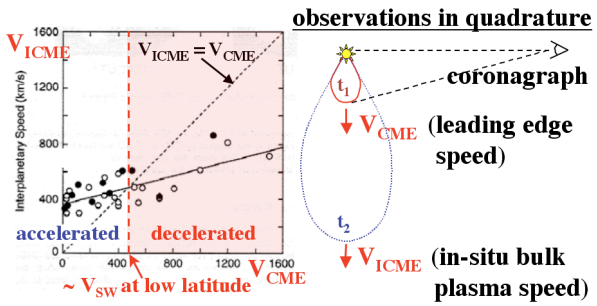

FIGURE 3. Evolution of the velocity of CMEs/ICMEs from the corona to the interplanetary medium with coronagraph and *in situ* observations in quadrature [Adapted from 7].

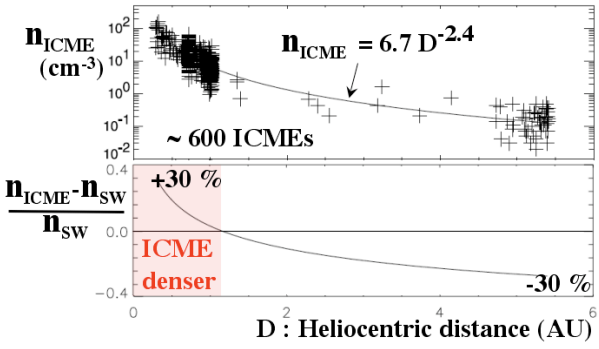

FIGURE 4. Evolution of the density of ICMEs versus the distance to the Sun. The lower panel shows the average evolution of the ICME density relative to the ambient SW density [Adapted from 8].

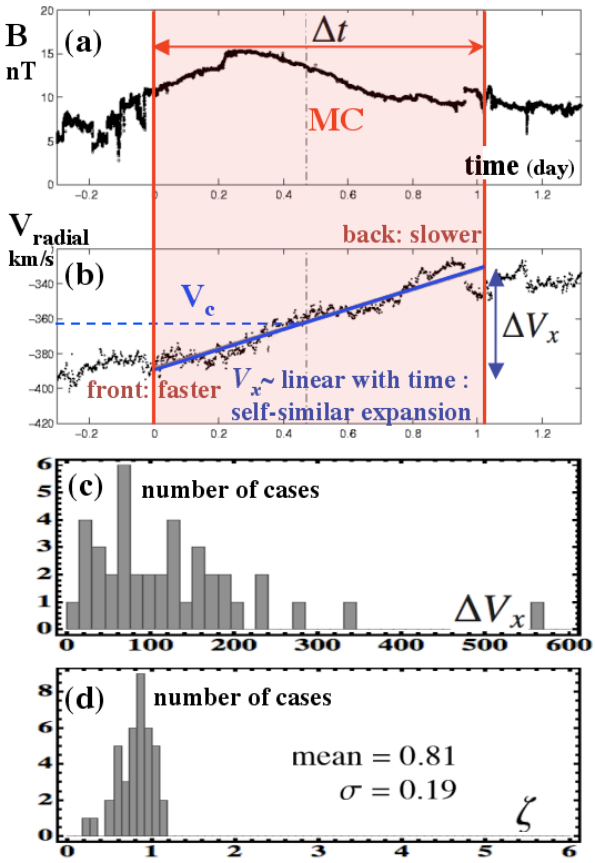

FIGURE 5. Field strength **(a)** and radial velocity **(b)** measured at 1 AU in a typical magnetic cloud (MC). The definition of the main quantities defining the undimensioned expansion parameter ζ are shown. Histograms of ΔV_x **(c)** and ζ **(d)** for unperturbated MCs (not overtaken by a fast stream or an ICME) [Adapted from 19].

medium, in particular their velocity (section 2), their expansion rate (section 3) and their shape (section 4). Like in the ocean, corsairs could be present, and some ICMEs are overtaken by a fast SW stream or by another ICME (section 5).

2. MODIFICATION OF THE ICME MEAN VELOCITY

One possibility to track an ICME is to follow its leading shock through its radio emission at the local plasma frequency or its harmonic ($\propto \sqrt{density}$, type II burst). Since the SW plasma density decrease as $\approx 1/D^2$, where D is the solar distance, the inverse of the radio frequency emitted is an estimation of D. Then, the shock propagation is followed by the drift in frequency [9, 10, 11].

Another way to track an ICME is to observe the associated CME with a coronagraph at the solar limb and the *in situ* ICME with a spacecraft in quadrature with the coronagraph (figure 3). This configuration was realized in several "lucky" cases in the past and more systematically presently with STEREO spacecraft [7, 12]. CMEs faster than their surrounding SW are typically decelerated (and the reverse for CMEs slower than the SW), implying a strong coupling (drag force) between the moving structure and the SW [7, 13, 14, 15].

Various drag forces have been investigated [16, 17]. Typically the strongest deceleration occurs close to the Sun, and ICMEs have a nearly constant velocity in most of the heliosphere [outward of 0.3 AU, 4, 8, 6]. A part of the drag force is due to the accumulation of the slower SW mass in front of the CME. For example, in an MHD simulation of a fast CME [18], the mass of the CME increases by a factor 5, inducing a decrease of a factor 3 of its mean velocity (from 1200 to $\approx$ 400 km/s).

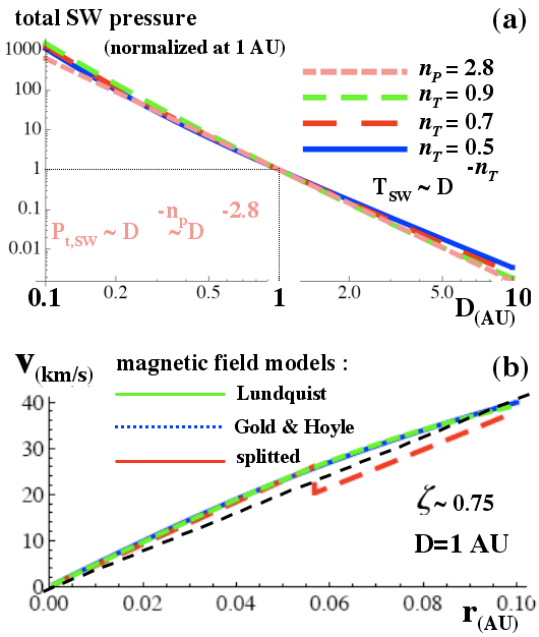

FIGURE 6. **(a)** Typical evolution of the total pressure present in the SW with radial distance to the Sun (D). **(b)** Results of a force-free flux rope models studying the evolution within a SW with a total pressure $\propto D^{-2.8}$. The expansion velocity, V, is nearly a linear function of the internal radius, r, independently of the magnetic field distribution, as observed in MCs (*e.g.* figure 5b) [Adapted from 20].

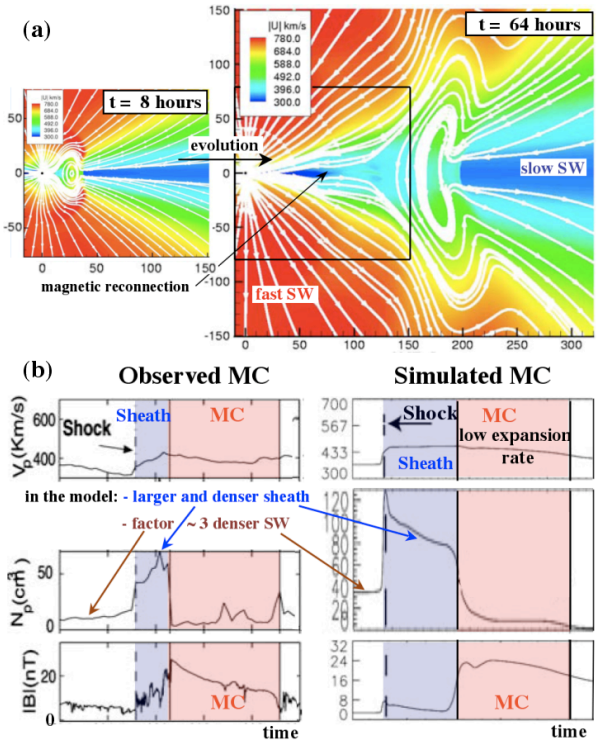

FIGURE 7. **(a)** 3D MHD simulation of a flux rope ejected from the Sun. The plots are in a meridional plane, orthogonally to the flux rope axis. The flux rope cross section is strongly distorted by the latitudinal velocity gradient present between the slow and fast winds. **(b)** Comparison between a typical MC observation at 1 AU and the above simulation. The simulation has been re-scale to have a similar mean velocity, size (so time duration) and maximum field strength as in the observed case [Adapted from 22].

3. EXPANSION RATE OF ICMES

The plasma density in ICMEs is decreasing with the solar distance, D, in average faster than in the SW (figure 4). The density within 0.3 to 5 AU decreases typically in between $D^{-2.3}$ and $D^{-2.6}$ [4, 8, 21], with the exception of the recent results of [6] obtained only with Ulysses. This implies that ICMEs have a 3D expansion in contrast with the SW with its approximative 2D expansion (with a nearly constant radial velocity for $D \geq 0.3$ AU). The expansion in the radial direction (away from the Sun) is detected *in situ* (figure 5b). ICMEs are in average denser than the SW in the inner heliosphere, while their over expansion implies that they becomes less dense than the SW outward (figure 4). Still, this is only a weak effect and this statistical property cannot be used to identify ICMEs in the SW.

The radial expansion velocity, ΔV_x, is defined by the difference of velocity between the front and the back. ΔV_x is highly variable from one event to another one, even for MCs traveling in a "quiet" SW. It ranges from un-significant values to a few 100 of km/s (figure 5c). However, a small fraction of MCs are in compression, while about half of MCs have strongly distorted velocity profile [far from linear with time, 23]. Typically such cases are overtaken by a fast stream or another ICME (section 5). A better characterization of the expansion (or compression) is achieved by defining a non-dimensional expansion factor $\zeta = (\Delta V_x/\Delta t) D V_c^{-2}$ (see the definition of the parameters in figure 5a,b). In contrast of the broad distribution of ΔV_x, the distribution of ζ is narrow for un-overtaken MCs (figure 5d), showing that all these MCs have a typical expansion rate. Moreover ζ is independent of the magnetic field strength, of D and of the size of the analyzed MCs [19, 23].

Why do MCs have a typical non-dimensional expansion rate? It is determined by the total pressure balance between the MC and the surrounding SW. Of course there is not an exact pressure equilibrium because, for example, of the magnetic tension, the evolution and the jump of pressure at the shock (if present). Still the pressure inside a MC can only be a few times larger than in the surrounding SW, while the SW pressure decreases by a factor $\approx 10^{-3}$ when D is multiply by a factor 10 (figure 6a). With magnetic flux conservation, this pressure

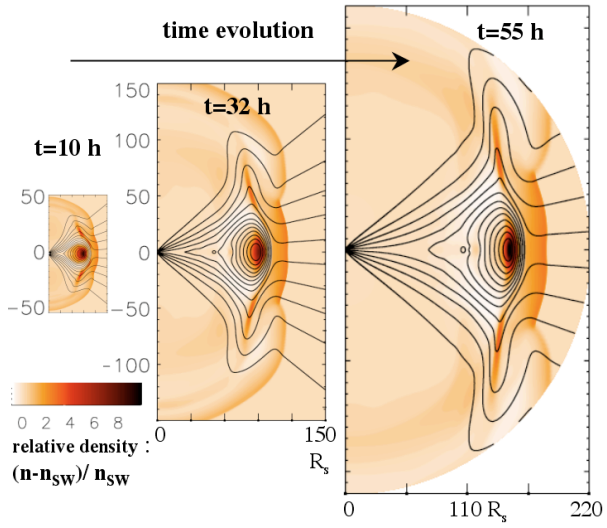

FIGURE 8. Axisymmetric 2.5D MHD simulation of a flux rope ejected from the Sun with a background SW as in figure 7. Differences in the flux rope set up close to the Sun lead to a different evolution of the flux rope cross-section [Adapted from 2].

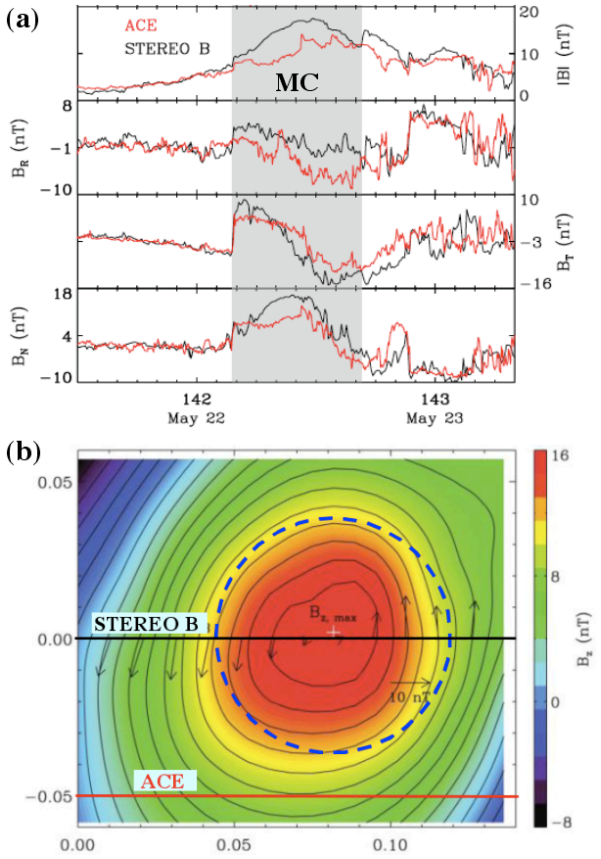

FIGURE 9. **(a)** Magnetic field strength and components observed by ACE and STEREO B across a MC. **(b)** Reconstructed cross section of the MC using STEREO B data and a 2.5D magnetostatic equilibrium within the MC moving frame. Black contours show the field lines projected orthogonally to the MC axis and the color shading indicates the value of the axial field. The trajectories of STEREO B and ACE, as well as a dashed circle, are superposed [Adapted from 24].

balance gives a flux rope radius increasing as $\approx D^{0.7}$. A more detailed flux rope model confirms this, and shows that the expansion rate is almost independent of the internal field model with conservation of magnetic flux or of magnetic helicity [so ideal or dissipative MHD, 20]. While worked out in detailed for MCs, these results are expected to extend to ICMEs from an on going research.

4. DEFORMATION OF THE FLUX ROPE

At the opposite of a ship, an ICME is a deformable structure. This is presently best studied with MHD numerical simulations with an unstable flux rope launched from the corona in a prescribed SW. In the simulations of [1, 22, 18], the flux rope is large enough to propagate both in the slow and fast wind (figure 7a). The gradient of velocity, so of dynamic pressure, induced a large deformation of the flux-rope cross section (set nearly circular close to the Sun).

The results of a numerical simulation can be compared to *in situ* observations by extracting the temporal evolution of the physical parameters at a fixed spatial location (figure 7b). The temporal profiles of velocity, density and field strength are comparable in the simulation and observations. Still, the sheath region (accumulated SW plasma and B field in front of the flux rope) is much larger and denser in the simulation. Indeed the density of the SW was set 3 times larger than the typical value present in the slow SW. This is one origin of the strong distortion and low radial expansion of the simulated MC.

Other authors found less deformed flux ropes (e.g figures 8,10). The main differences with the simulation of figure 7 are a different initial flux rope and axisymmetric simulations. In figure 8, mostly the lateral borders of the flux rope and the encounter SW fields are severely distorted into two lateral extensions. If a spacecraft would cross one of such extensions, it would detect some characteristics of an ICME (*e.g.* an enhanced B field), but without the full characteristics of a MC. This is a case where the flux rope detection would be missed. We presently do not know which fraction of non-MC ICMEs have a flux rope.

In situ observations indicate that some MCs can be flat [*e.g.* 25], but very flat configurations, such as in figure 7, are rather exceptional. Research of such bended flux ropes have, so far, not been successful [26]. Indeed,

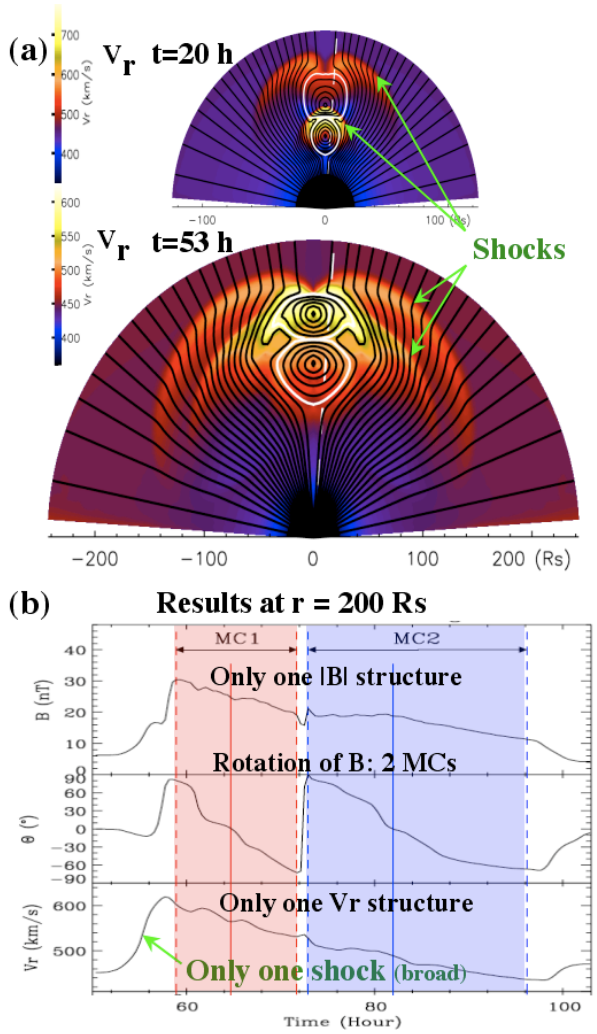

FIGURE 10. **(a)** Axisymmetric 2.5D MHD simulation of the interactions of two parallel flux ropes with the same characteristics and launched from the same part of the Sun with a time difference $\approx$ 12h. The color shading shows the radial velocity. **(b)** Time evolution of the magnetic field magnitude and latitude (θ), and of the radial velocity computed at a fixed spatial position. The two flux ropes are detected only on the orientation of the magnetic field (θ) as observed in the case shown in figure 11a [Adapted from 3].

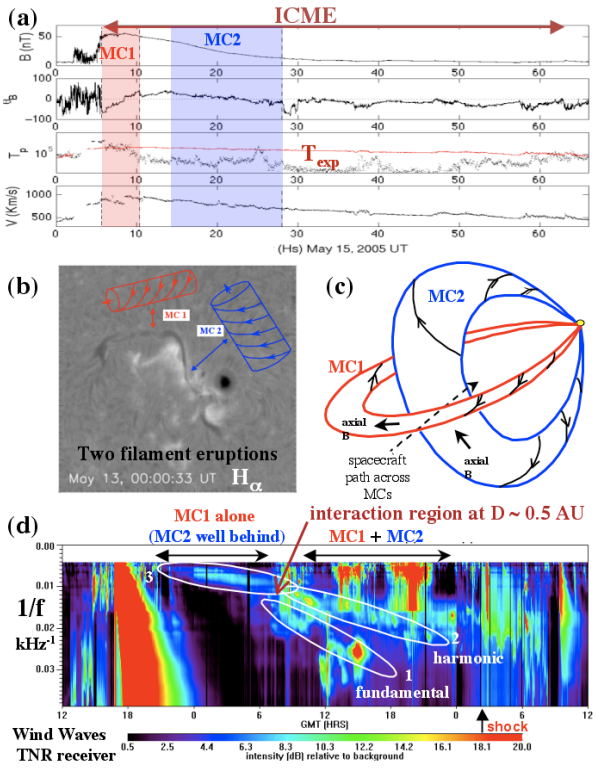

FIGURE 11. **(a)** *In situ* observations of an ICME with two interacting MCs inside. **(b)** The eruption of two filaments are the solar sources of the MCs. The sketches of the flux ropes are added; there orientations, deduced from *in situ* observations, are comparable to the related filament orientations. **(c)** Sketch of the interacting flux ropes. **(d)** Dynamic spectral plot showing the radio emission of the interplanetary shocks (type II burst) in front of the ICME (encircled regions) [Adapted from 28].

recent results of STEREO and ACE, together with modelization, figure 9, rather indicates a relatively round core [24, 27].

5. OVERTAKEN ICMES

During its outward travel, an ICME can be overtaken by a faster one [29, 30, 31]. This has been simulated by the launch of two successive flux ropes in numerical simulations similar to the ones described in previous section [32, 3, 33]. A simple example with two identical flux ropes and with negligible reconnection is shown in figure 10a. The shock of the second flux rope first reaches the first flux rope, then crosses it rapidly, to finally merges with the first shock (figure 10a). Then, the first flux rope is compressed by the second flux rope, so the first one is flatter and also smaller (at a fixed solar distance). After this interaction they travel together as one entity.

Similar cases have been observed, but with flux ropes having different orientations and B flux [*e.g.* 28]. In the ICME shown in figure 11, two MCs have been identified, in particular by the two different coherent regions of the magnetic field latitude (θ_B in figure 11a). The solar sources have been identified as two filament eruption from the same active region (figure 11b). The shock in front of the first MC has been track through its radio emission (figure 11d). The shock has a significant change of velocity around $\approx$ 0.5 AU, locating the time of contact between the two MCs (in agreement with the timing of

the eruption and the *in situ* measured velocities of the MCs).

The overtaking ship can also be a fast SW stream. This is detected *in situ* by a fast velocity observed behind the MC, but also inside a significant part of the MC [23]. As expected most the overtaken MCs have a significant slower expansion rate (lower ζ value) than non-overtaken ones (figure 5d). Still, surprisingly, a few expand faster! In fact, the overtaking process is a time dependent process. Firstly, the MC is compressed. Secondly, the fast SW over pass the MC from the sides. Finally, the MC has a too high internal pressure compare to the surrounding SW (section 3), so it expands faster to catch up with the internal pressure and size it would have reached without interaction.

6. CONCLUSION

There are many interaction processes between ICMEs and the SW. Only four are reviewed above. These interactions modify the ICME mass and mean velocity, but also define the expansion rate and the shape of ICMEs. There is also magnetic reconnection between ICMEs and the overtaken SW field (called interchange reconnection). This modifies two other global ICME quantities: its magnetic flux and helicity contain [34, 35, 36]. It also progressively remove the ICME magnetic connections to the Sun and play an important role in reshaping the heliospheric field [37, 38]. So the interaction with the SW indeed affects the main ICME physical properties. As ICMEs are moving away from the Sun they progressively loose their identity [*e.g.* 6]. More over ICMEs interact between them, forming complex structures with increasing solar distance.

REFERENCES

1. W. B. Manchester, T. I. Gombosi, and I. Roussev, *et al.*, *J. Geophys. Res.* **109**, A01102 (2004).
2. E. Chané, B. Van der Holst, C. Jacobs, S. Poedts, and D. Kimpe, *Astron. Astrophys.* **447**, 727–733 (2006).
3. M. Xiong, H. Zheng, S. T. Wu, Y. Wang, and S. Wang, *J. Geophys. Res.* **112**, A011103 (2007).
4. Y. Liu, J. D. Richardson, and J. W. Belcher, *Planetary Spa. Sci.* **53**, 3–17 (2005).
5. R. F. Wimmer-Schweingruber, N. U. Crooker, A. Balogh, and et al, *Space Sci. Rev.* **123**, 177–216 (2006).
6. R. W. Ebert, D. J. McComas, H. A. Elliott, R. J. Forsyth, and J. T. Gosling, *J. Geophys. Res.* **114**, A01109 (2009).
7. G. M. Lindsay, J. G. Luhmann, C. T. Russell, and J. T. Gosling, *J. Geophys. Res.* **104**, 12515–12524 (1999).
8. Y. Wang, P. Ye, G. Zhou, S. Wang, S. Wang, Y. Yan, and J. Wang, *Solar Phys.* **226**, 337–357 (2005).
9. D. B. Berdichevsky, C. J. Farrugia, and B. J. Thompson, *et al.*, *Annales Geophysicae* **20**, 891–916 (2002).
10. M. J. Reiner, M. L. Kaiser, and J.-L. Bougeret, *Astrophys. J.* **663**, 1369–1385 (2007).
11. S. Hoang, C. Lacombe, R. J. MacDowall, and G. Thejappa, *J. Geophys. Res.* **112**, A09102 (2007).
12. A. P. Rouillard, *this issue* (2009).
13. N. Gopalswamy, A. Lara, S. Yashiro, M. L. Kaiser, and R. A. Howard, *J. Geophys. Res.* **106**, 29207–29218 (2001).
14. J. Zhang, K. P. Dere, R. A. Howard, and V. Bothmer, *Astrophys. J.* **582**, 520–533 (2003).
15. R. Schwenn, A. Dal Lago, E. Huttunen, and W. D. Gonzalez, *Annales Geophysicae* **23**, 1033–1059 (2005).
16. B. Vršnak, *Annales Geophysicae* **26**, 3089–3101 (2008).
17. A. Borgazzi, A. Lara, E. Echer, and M. V. Alves, *Astron. Astrophys.* **498**, 885–889 (2009).
18. N. Lugaz, W. B. Manchester, IV, and T. I. Gombosi, *Astrophys. J.* **627**, 1019–1030 (2005).
19. P. Démoulin, M. S. Nakwacki, S. Dasso, and C. H. Mandrini, *Solar Phys.* **250**, 347–374 (2008).
20. P. Démoulin, and S. Dasso, *Astron. Astrophys.* **498**, 551–566 (2009).
21. M. Leitner, C. J. Farrugia, C. Möstl, K. W. Ogilvie, A. B. Galvin, R. Schwenn, and H. K. Biernat, *J. Geophys. Res.* **112**, A06113 (2007).
22. W. B. I. Manchester, T. I. Gombosi, I. Roussev, A. Ridley, D. L. De Zeeuw, I. V. Sokolov, K. G. Powell, and G. Tóth, *J. Geophys. Res.* **109**, A02107 (2004).
23. A. M. Gulisano, P. Démoulin, S. Dasso, M. E. Ruiz, and E. Marsch, *this issue* (2009).
24. Y. Liu, J. G. Luhmann, K. E. J. Huttunen, R. P. Lin, S. D. Bale, C. T. Russell, and A. B. Galvin, *Astrophys. J.* **677**, L133–L136 (2008).
25. M. Vandas, E. P. Romashets, and S. Watari, "Connecting Sun and Heliosphere," in *Fleck, B., Zurbuchen, T.H., Lacoste, H. (eds.), Solar Wind 11 / SOHO 16, ESA SP-592, 159.1 (on CDROM)*, 2005.
26. M. J. Owens, *J. Geophys. Res.* **111**, A12109 (2006).
27. C. Möstl, C. J. Farrugia, H. K. Biernat, M. Leitner, E. K. J. Kilpua, A. B. Galvin, and J. G. Luhmann, *Solar Phys.* **256**, 427–441 (2009).
28. S. Dasso, C. H. Mandrini, and B. Schmieder, *et al.*, *J. Geophys. Res.* **114**, A02109 (2009).
29. L. F. Burlaga, R. M. Skoug, C. W. Smith, D. F. Webb, T. H. Zurbuchen, and A. Reinard, *J. Geophys. Res.* **106**, 20,957–20,977 (2001).
30. Y. M. Wang, S. Wang, and P. Z. Ye, *Solar Phys.* **211**, 333–344 (2002).
31. C. Farrugia, and D. Berdichevsky, *Annales Geophysicae* **22**, 3679–3698 (2004).
32. N. Lugaz, W. B. Manchester, IV, and T. I. Gombosi, *Astrophys. J.* **634**, 651–662 (2005).
33. N. Lugaz, *J. Atmos. Sol. Terr. Phys.* **70**, 598–604 (2008).
34. S. Dasso, C. H. Mandrini, P. Démoulin, and M. L. Luoni, *Astron. Astrophys.* **455**, 349–359 (2006).
35. S. Dasso, M. S. Nakwacki, P. Démoulin, and C. H. Mandrini, *Solar Phys.* **244**, 115–137 (2007).
36. P. Démoulin, *Annales Geophysicae* **26**, 3113–3125 (2008).
37. N. U. Crooker, R. Forsyth, A. Rees, J. T. Gosling, and S. W. Kahler, *J. Geophys. Res.* **109**, A06110 (2004).
38. N. U. Crooker, and T. S. Horbury, *Space Sci. Rev.* **123**, 93–109 (2006).